Effects of Briquettes with Different Crack Structures on Propagation Characteristics of Ultrasonic Waves under Wetting Conditions

Gang Wang (gang.wang@sdust.edu.cn)
Shandong University of Science and Technology https://orcid.org/0000-0003-4742-8103
Jinzhou Li
Shandong University of Science and Technology
Huaixing Li
Shandong University of Science and Technology
Zhiyuan Liu
Shandong University of Science and Technology
Yanpei Guo
Shandong University of Science and Technology
Xianglan Liu
China Coal Technology and Engineering Group Corp China Coal Research Institute

Research

Keywords: Artificial cracks, Wetting height, Ultrasonic wave, Propagation characteristics, Briquette

Posted Date: September 11th, 2020

DOI: https://doi.org/10.21203/rs.3.rs-72803/v1

Abstract

In order to examine the effect of briquettes with different crack structures on ultrasonic characteristics under different wetting conditions, a series of ultrasonic testing are carried out on briquettes at different wetting heights and the ultrasonic characteristics in these coal samples are explored. The results show that ultrasonic amplitude is positively correlated with the emission voltage, whereas ultrasonic frequency is negatively correlated with the emission voltage. Changes in both are closely related to the particle size and density. The ultrasonic velocity is positively correlated with the wetting degree. Sample mass has the greatest effect on the ultrasonic velocity, followed by particle size, and pressure has the smallest effect. At dry stage, ultrasonic velocity in gas coal is less than that in bituminous coal. The opposite is true in the fully wet state. The influence of crack thickness on ultrasonic velocity gradually increases with the wetting degree increasing. At dry stage, the velocity gradually increases with the crack dip increasing, while as the wetting height increasing, magnitude of velocity increase gradually decreases with the dip increasing. The ultrasonic attenuation in the briquettes reduces with the emission voltage enhancing. The attenuation decreases with sample particle size, crack thickness and crack size decreasing and with sample mass, pressure and crack dip increasing. The ultrasonic attenuation shows a trend of increase before decrease with the wetting height increasing. The attenuation of ultrasonic wave increases with wave velocity increasing for intact samples and shows a trend of increase before decrease for cracked samples.

1. Introduction

Coal rocks are heterogeneous media containing a large amount of pores and microcracks. As a special porous, saturated fluid mixture, water-bearing coal rocks are widely presented in the rock formations (Alexeev et al., 1999; Wang et al., 2018; Liu et al., 2015; Zhang et al., 2001). Due to the presence of water in these pores and microcracks, compared with dry coal samples, water-bearing coals possess quite different characteristics. The effects of water in coal rocks on their physical and mechanical characteristics have been an important research topic and drawn great attentions in coal mining and earthquake prediction. The ultrasonic testing technology for coal rock media is used to study the mechanic properties and structural features of coal rocks by measuring the changes in acoustic parameters such as wave velocity, attenuation coefficient, amplitude, etc. of ultrasonic signals passing through the coal rocks base on the information carried by ultrasound waveforms (Wang et al., 2015). Since porous structure and water content are two important factors impacting ultrasonic testing, experimental observation and analysis of coal rock samples with different porous structure and water content can provide an experimental basis for researches on underground water injection in coal mines.

In recent years, scholars have carried out numerous experimental and theoretical studies to establish the relationship of physical and mechanical properties of coal rock to ultrasonic signals and made significant achievement and progress. For example, Shea-Albin et al. employed the MTS servo-controlled rock testing system to conduct uniaxial and triaxial experiments on coal samples in Utah, USA (Shea and Hanson, 1988). They found that the ultrasonic velocity and attenuation characteristics can be used as

indicators to reflect the load change and structural integrity of coal mass and concluded that the velocity and attenuation of the transverse wave clearly can reflect the axial load variation of coal samples before failure and the initial developmental conditions of microcracks than those of the longitudinal wave. Prasad and Manghnani studied the longitudinal wave attenuation anisotropy in Berea sandstone and Michigan sandstone (Prasad and Manghnani, 2002). Fener found that changes in sound velocity in rocks with porosity of 0–25% were governed mainly by porosity and followed by the ratio of carbonate to silicate plastic materials (Fener, 2011). Gaviglio established the relationship between ultrasonic velocity and coal density (Gaviglio, 1989). Pyrak-Nolte et al. derived the theoretical velocity of waves propagating in coal rocks based on the displacement discontinuity model (Pyrak-Nolte and Myer, 1987). Zhao et al. developed an equivalent medium method to explain wave phenomenon (Zhao et al., 2006). Cai and Zhao established and modeled the effects of multiple parallel planar cracks on the attenuation of one-dimensional elastic waves that were normally incident on the planar cracks(Cai and Zhao, 2000). Mashinskii found that wave attenuation was improved by including it in the seismic rheological model (Mashinskii, 2013). Fan et al. proposed a non-linear viscoelastic medium equivalent model to simulate the propagation of longitudinal stress waves in rock masses and found that the propagation of waves in complex rock masses was not always attenuated but may actually be enhanced in some cases(Fan et al.,2012; Fan and Sun ;2015, Fan et al., 2018). Ma et al. evaluated the existing equivalent medium methods for stress wave propagation in jointed rock masses, based on which, they further developed an equivalent viscoelastic medium method(Ma et al., 2013). In addition, some scholars also established the relationship between ultrasound and water content in coal rock masses. Hudson et al. and Liu et al. separately discussed different effective medium theories and determined the fracture size, porosity, and relative permeability of fluid-saturated materials with their fractures aligned with longitudinal wave (Hudson et al., 2001 ; Liu et al., 2015). Mahoney et al. studied the dependence of coal grade and lithology on coal wettability, which provided a basis for the improved relative permeability model (Mahoney et al., 2017). Recently, Liu explored the relationships of water saturation, porosity, permeability, micro-cracks as well as coal grade to longitudinal wave velocity with focus on quantitatively measuring the relationship between water saturation and longitudinal wave velocity by nuclear magnetic resonance (Liu et al.,2017). Valès et al. established the relationship between different mechanical parameters (elasticity and failure data) and samples' water saturation, and found that the mechanical behavior of shale is very sensitive to its water saturation state and the direction of its mechanical stress (Lebedev et al., 2015). Wang et al. carried out ultrasonic testing experiments on anthracite, coking coal, and fat coal samples in dry and naturally saturated water absorption states, analyzed ultrasonic signals and studied the ultrasonic characteristics. They found that the longitudinal wave velocities in different coal samples have different sensitivities to water and the wave velocity and principal frequency of ultrasonic signals can reflect the pores, microcracks and other structural conditions as well as the water content in coal samples (Wang et al., 2018).

Overall, the physical characteristics of fractured rock masses have been extensively studied These studies not only expound the propagation and attenuation laws of ultrasonic waves in different types of fractures, but also reveal the relationships of ultrasonic characteristics to different water-bearing rocks.

However, very few studies have jointly investigated the attenuation effect of cracks on ultrasonic waves and the relationship of ultrasonic characteristics to water content in coal rocks. Therefore, to implement a joint study on ultrasonic characteristics, coal rock water content, and pore-crack structure, in this study, we first prepared briquette samples with different crack structures (crack size, number, openness, and angle), then used the I-RPT ultrasonic testing instrument to measure the velocity of high-frequency ultrasonic pulses through coal samples and acquired the experimental data of longitudinal wave characteristics of coal samples under different conditions, and investigated the relationships of longitudinal wave characteristics (frequency, wave velocity, attenuation) to different humidity, mass, particle size,pressure, cracks in coal rock samples.

2. Experimental Methods

2.1 Coal sample preparation

Raw coals for briquette preparation used in this experiment were collected from Tangkou Coal Mine and Liangbaosi Coal Mine in Nanzhang Town, Rencheng District, and Liangbaosi Town, Jiaxiang County, respectively, in Jining City, Shandong Province, China, as well as Gaojiabao Coal Mine in Dizhang Town and Penggong Town, Changwu County, Xianyang City, Shaanxi Province, China, as shown in Fig. 1. Briquette samples wee prepared as follows: 1) select large, hard, raw coal bulks with good homogeneity from underground coal mines strictly following the international sampling standards; 2) pulverize these coal bulks using a coal crusher into coal powder with sizes of 20–40 meshes, 40–80 meshes, and 80–120 meshes, respectively; 3) place certain amount of coal powders into the molds and press them for 30 min using a hydraulic presser the required height; and 4) take out the pressed samples for testing. Figure 2 shows the procedure of briquette preparation.

2.2 Longitudinal velocity testing

Ultrasonic pulse transmission technique is one of the most commonly used non-destructive methods (Birch, 1961; Pyrak-Nolte et al.,2004 ; Cadoret et al., 1995; Gebrande,1982; Ciccotti et al., 2004). According to the relevant content of "Specification for Measurement of Rock Acoustic Properties in Laboratory", the technique is used in this study to examine the propagation of ultrasonic waves in coal rock with an ultrasonic testing system, as shown in Fig. 3. The ultrasonic test system consists of a pair of longitudinal wave transducers, an I-RPT ultrasonic tester with transducer frequency of 50 kHz, acoustic timing accuracy of ± 0.5 μs, and gain accuracy of 3%, a transducer holder, and a PC for data acquisition. A briquette sample is held in between two well-connected sensors to the interface by using the Moco 7501 high vacuum silicone grease. In order to make the sample end surfaces better coupled with the sensors, a holder is used to clamp the transducer and the sample with the same force each time. The experiment is conducted at room temperature, about 20 °C as described follows:

1) Measure the size of briquette samples using a Vernier caliper, 2) Dry the samples at 105 °C in a vacuum oven for 24 h, measure their mass and size, and labeled the results as and M_{dry} and S_{dry}, 3)

Detect the velocity of ultrasonic waves passing through the dried sample after fixing the transducer at the center of two ends of the sample, and record the tested results, 4) Immerse the samples into water at 1/5, 2/5, 3/5, 4/5 and 5/5 of the height, respectively, for the same time, 5) Weigh the wetted samples, subject the samples to ultrasonic testing, 6) Record and analyze the results. The measured sample length L and the measured time T of ultrasonic wave passing through the sample are used to find the wave velocity based on the following formula:

$$V = L/T \quad (1)$$

where V is the ultrasonic velocity, m/s; L is the sample length, m; and T is the ultrasonic propagation time in the sample, s.

3. Results Analysis

3.1 Relationships of voltage to amplitude and frequency

The propagation of ultrasonic waves in coal samples is affected by many impacting factors. Among them, the emission voltage of the acoustic wave probe will influence the distribution of the ultrasonic field, and subsequently affect the propagation of acoustic waves in the coal sample. In this experiment, the briquette samples from the Tangkou Coal Mine is subjected to the ultrasonic testing experiments at emission voltage of 60v, 125v, 250v, 500v, and 1000v, respectively.

Fig.4 shows the ultrasonic spectra of briquettes prepared under different conditions. From the figure it is clearly that the principal frequency of ultrasonic signals shows a decrease trend as the mass of briquettes as well as the size of coal grains increase, while shows an increase trend as the pressure rises. In general, the principal frequency undergoes a frequency shift under different experimental conditions, among which, the amplitude of principal frequency drop is the greatest at different pressures, indicating that the principal frequency of ultrasonic signals is most affected by pressure, followed by the coal granularity and the briquette mass in order.

Fig.5 shows the dependence of different emission voltages on acoustic amplitude and frequency. From Fig.5(a) it can be seen that the principal frequencies of acoustic waves drops at different emission voltages when passing through briquettes with masses of 250 g, 270 g, and 290 g. At different emission voltages, the amplitude of principal frequencies of acoustic waves decreases the most for briquette with mass of 250 g, and the least for briquette with mass of 290 g. The results indicate that under different voltage conditions, briquette with higher mass has less effect on the principal frequency, *vice versa*. On the contrary, the amplitude of acoustic waves shows an increase trend at different emission voltages, which is more obvious in briquette with higher mass. Overall, the amplitude of acoustic waves is positively correlated with the emission voltage. From Fig.5(b) it is not difficult to see that for briquettes prepared with coal powder with different sizes, at different emission voltages, the principal frequency of transmitted ultrasonic waves shows a consistent downward trend. By contrast, the amplitude shows a consistent, upward trend. The amplitude of acoustic waves is the highest for briquettes prepared with

coal powder with 80–120 meshes, while the principal frequency drops the largest. Similarly, the principal frequency of transmitted acoustic waves shows a decline trend with the voltage increasing, whereas the amplitude shows a rise trend. Among theses briquettes, the amplitude is the highest at the largest pressure, while principal frequency drop is roughly same.

3.2 Effects of different wetting heights on acoustic velocity

If water is stored in the pores and microcracks of water-bearing coal samples, their characteristics will change compared to those of dry samples(Meng et al., 2004; Han et al., 2020; Liu et al., 2004; Liu et al., 2020). Therefore, studying the effect of water content in coal on coal's acoustic parameters has certain practical significance for understanding the physical and mechanical characteristics of coal rocks. So far, the conclusions of studies on the influence of moisture on the ultrasonic parameters of coal rocks are discrepant. In this experiment, briquette specimens prepared with different mass and particle size at different pressure are utilized to preliminarily explore the influences of coal humidity on the ultrasonic velocity and to explain the behavior of ultrasonic propagation in the coal samples of different water contents. In the experiments, the immersion height is used to describe the wetting range of coal samples for studying the relationships of the wetting range of coal samples to the ultrasonic velocity under different conditions.

As we all know, an ultrasonic tester could send ultrasonic pulse signals to the samples, receive the pulse signals passing through the test piece and record the time needed for ultrasonic wave through the sample, waveform and amplitude of the received acoustic waves, as shown in Fig.6. The ultrasonic velocity can be calculated according to the time needed for ultrasonic wave passing through of a sample with certain length, and the energy attenuation of ultrasonic pulses can be obtained according to the amplitude change of wave propagating through the sample. Generally, the head wave is the first arrival acoustic signal (Liu et al., 2019). Fig.7 shows the oscillograms of the ultrasonic head waves. From the figure, it is clear that the arrival time of the acoustic head wave through the briquettes with different water-immersing heights varies, with the immersing height rising, the arrival time of the head wave shortens gradually. In this study, the wave velocity for each briquette, as shown in Fig.8 was obtained according the head wave oscillogram shown in Fig.7(c).

From Fig.8, obviously, the overall velocity shows an increase trend with wetting height increasing at different mass, granularity and pressure conditions. For samples with different mass, wave velocity is similar at dry conditions, but varies greatly at different wetting conditions, showing greater difference in samples with higher mass with the wetting height continuously increasing and the highest difference for the briquette with mass of 290 g. For samples with different particle sizes, the difference in wave velocity is more obvious at dry conditions and gradually narrows with the wetting height continuously increasing and becomes close to zero at fully immersed state. It is worth mentioning that the wave velocity of briquette with particle size of 20–40 meshes is higher at fully immersed state than at dry state, and becomes the highest among the samples with three particle sizes. This may be due to different porosity of the three samples. Because the samples with 20–40 meshes have the largest porosity, their water

bearing capacity is also the highest. High water content makes the briquette become more homogeneous, leading to increased wave velocity. Under different pressures, clearly, wave velocity increases with the increase of pressure at dry condition and changes similarly with wetting height increasing. Overall, in the wetting process, an increase in mass makes the difference in wave velocity greater and greater, showing the greatest difference in the sample with mass of 290 g. Although the particle size does not significantly increase the wave velocity difference, it is the factor making the wave velocity of briquette with greatest porosity higher at fully immersed state than at dry state, indicating that the granularity of the coal samples is more sensitive to wave velocity. The effect of pressure on the test pieces is the smallest. Thus, the wave velocity of briquettes at different pressures increases similarly with wetting height increasing.

To further explore the effects of coals from different sources on the ultrasonic wave velocity under different wetting conditions, the acoustic wave velocity of briquettes with mass of 270 g prepared from raw coals of 40–80 meshes from Tangkou Coal Mine, Liangbaosi Coal Mine, and Gaojiabao Coal Mine was tested at pressure of 15 MPa. The results are shown in Fig.9.

It is clear from Fig.9 that the wave velocity of the three samples increases with the increase of the wetting height, but their changing trends are different. At the dry state as shown in Fig.9(a), the wave velocity is the highest, 0.72 km/s, in samples from Tangkou, followed by that of 0.69 km/s in samples from Liangbao, and the smallest of 0.56 km/s in samples from Gaojiabao. In the wetting process, the wave velocity in the samples from Gaojiabao reaches its peak at wetting height of 1/5 and remains stable afterward. By contrast, the wave velocity in samples from Tangkou and Liangbao shows a roughly similar trend of increase after decrease with peak at wetting height of 3/5, as shown in Fig.9(b). The coal samples from Tangkou and Liangbaosi are gas coals. Although their geographical locations are different, their trends are alike. Compared with the other two, samples from Liangbaoshi are bituminous coal. Thus, the trend of wave velocity change is different from the other two. Coals with higher metamorphic degree often have low water adsorbing, which may attribute to the above phenomenon.

3.3 Effects of different crack thickness and size on wave velocity

Coal has a complex fracture structure and often forms joints during the coal formation process. As the basic characteristics of coals, they have great impacts on the propagation of elastic waves in coal bodies, making the velocity of seismic waves decrease but the wave attenuation increase. However, because joints and cracks often have different orientations, their influences on wave propagation also differ greatly. The aim of researches on the ultrasonic velocity in coals with different fractures at different wetting conditions is to explore the relationship between the difference in acoustic velocity with crack size and openness so as to provide an experimental basis for monitoring the water injection range of coal seams. In this experiment, the pulverized coal of Tangkou Coal Mine with a particle size of 40–80 meshes is utilized and mica flakes to simulate cracks in the sample. Fig.10 shows the ultrasonic test results.

It can be seen from Fig.10(a) that at dry state, the wave velocity of samples with different crack openness is roughly the same. Among them, the sample with four layers of mica flakes has the lowest wave

velocity, and the sample with only one layer of mica flake has the biggest wave velocity. The results are consistent with the theoretical results, indicating that mica flakes could well simulate artificial cracks and reflect the facts to a certain extent. With the continuous increase of the layer of mica flakes, the openness of artificial cracks also enlarges, making the medium of the specimen no longer continuous. The reason is that, the increase of the artificial crack openness will, on one hand, increase the obstacle against the ultrasonic propagation process, causing energy loss; on the other hand, provide a larger space for air present in the sample. Because ultrasonic waves propagate significantly lower in the air than in solids and liquids, large crack openness will reduce the propagation velocity of ultrasonic waves. With the continuous increase of the wetting height, the wave velocity of the samples increases, showing a positive correlation on the whole. It is worth mentioning that the wave velocity increases differently in these samples, showing slower increase rate in samples with one or two layers of mica flakes, both of which have similar increasing curves. By contrast, the wave velocity increase is greater in samples with three or four layers of mica flakes, and the increasing amplitude in the samples with four layers of mica flakes is greater than that in the samples with three layers of mica flakes, indicating that the increasing amplitude of the wave velocity enhances with the increase of the artificial crack openness. In the wetting process, as external water gradually reaches the artificial crack position. The presence of water not only enhances the propagation velocity of waves, but also increases the continuity of the medium and reduces the attenuation of ultrasonic energy, in other words, increases the wave velocity. A larger crack opening provides more room for water to improve the continuity of the coal sample. From Fig.10(b) it is clear that the changes in wave velocity of samples with different crack sizes show similar trends at both dry and wetting processes, indicating that the effect of crack size on wave velocity is small.

3.4 Effects of different crack dips on ultrasonic wave velocity

Coal rock is sedimentary rock of high molecular biopolymer with a large amount of defects like pores, cracks, and bedding and obvious heterogeneity and anisotropy (Ai et al., 2015). The bedding is the most widely developed structure in the coal seam. Its existence will destroy the continuity and integrity of coal mass and change the stress distribution in coal seams, making it the main factor controlling the coal strength, deformation and permeability (Pan et al., 2014). Based on this, the effects of cracks of different dips in coal samples on the ultrasonic velocity are examined at different wetting heights. Fig.11 schematically shows the artificial cracks with different dips in the coal samples.

As shown in Fig.12, the longitudinal wave velocity of all samples with a crack dip from 0° to 90° shows a roughly same trend. With the humidity of samples continuing to grow, the longitudinal wave velocity enlarges accordingly. It is worth noting that as shown in Fig.12, the wave velocity has a certain bedding effect. At dry state, as the crack dip increases from 0° to 90°, the ultrasonic wave velocity is continuously increasing from 0.56 km/s to 0.72km/s.

In terms of meso-structure, the bedding distribution is characterized by the difference in the distribution of matter and structure. This anisotropy in structure and matter compositions will, to a certain extent, make the propagation of ultrasonic waves in coal samples behave differently. For the specimen with a crack

angle of 90°, the extension direction of the crack surface is consistent with the direction of wave propagation. Therefore, the reflection of ultrasonic waves on the crack structure surface will greatly reduce the refraction effect. For the specimen with a crack angle of 0°, because the fracture structure surface is perpendicular to the direction of wave propagation, ultrasonic waves almost experience the mirror reflection on the fracture surface, reflecting a large number of waves or consuming a large amount of energy, which will result in a reduction in wave transmission capacity and velocity (Xu et al., 2015).

In terms of wave propagation mechanisms, when ultrasonic waves propagate in a sample, a part of its mechanical energy is converted into thermal energy. During this process, various mechanisms are collectively called internal friction (Chen et al., 2015). Both the reflection and refraction of ultrasonic waves on the bedding surface will cause internal friction and dissipate part of energy, resulting in a decline in the ability of ultrasonic waves to propagate. With a change in the crack dip, equivalent to a change in the incident angle, ultrasonic waves are constantly refracted and reflected between the fracture surfaces. With the angle of incidence increasing, the times of refraction and reflection of ultrasonic waves between the bedding planes will increase. Thus, the dissipated energy enlarges accordingly, resulting in a reduction in the transmission capacity of ultrasonic waves, and in a prolongation in the duration passing the sample. Thus, according to the velocity relation, the ultrasonic wave velocity will decrease.

As shown in Fig.13, in the conditions of fully water saturated coal samples, as the crack dip changes from 0° to 90°, the increment in ultrasonic wave velocity decreases consecutively from 0.47 km/s to 0.29 km/s in order. As stated above, the appearance of cracks affects the ultrasonic waves velocity and the presence of water strengthens the molecular activity, all of which provide good medium conditions for the propagation of longitudinal waves, increase the stiffness of pores and cracks, reduce the anisotropy of coal to a certain extent and make the coal body more uniform in its interior. All these indicate that the stronger the anisotropy of the sample is, the stronger the ability of water to weaken the anisotropy, which also explains the cause for this phenomenon.

3.5 Effects of different voltages on ultrasonic decaying

Like in other media, ultrasonic waves propagate in coal rocks and undergo geometric and physical attenuation. Ultrasonic waves experience scattering, refraction, heat loss, and other physical phenomena on the structural surfaces of different mechanical properties in the coal body, making the elastic wave energy continuously attenuated and the wave velocity clearly reduced. Analyzing the attenuation mechanism of ultrasonic wave propagation in coal finds that viscous friction on the boundaries of mineral particles and the surface of microcracks as well as the scattering effect of macrocracks are the main mechanisms causing wave attenuation (Li et al., 2015). The inelastic attenuation rate of ultrasonic vibration or wave energy in the medium is characterized by the attenuation coefficient. Briquettes made of coals from Tangkou Coal Mine are used as the experimental examples and the attenuation coefficient is calculated using the signal comparison method. On the premise that the consistent pressure, temperature, coupling, and other test conditions are fully ensured, the amplitudes of ultrasonic head waves are respectively measured and recorded when the transmitting and receiving transducer probes are

docked with the test sample. The attenuation coefficient is calculated in accordance with the following formula (Chen et al., 2012):

$$\alpha = (\ln A_0 - \ln A)/L \quad (2)$$

where α is the attenuation coefficient, dB/mm; A_0 and A are the amplitudes of ultrasonic head waves measured by the sensor probes at the emitting and receiving ends, respectively, dB; and L is the length of the test sample, mm.

Fig.14 shows the dependence of ultrasonic attenuation upon voltage at different experimental conditions. It is clear that the attenuation coefficient of ultrasonic wave decreases to some extent with the increase of the emission voltage. However in addition to the emission voltage, its attenuation is also affected by different briquette structural parameters. From Fig.14(a), as the mass of the sample increases, the ultrasonic attenuation coefficient continues to decrease, showing a close correlation with the density of samples with same size. From Fig.14(b), as the particle size of the sample increases, the ultrasonic attenuation coefficient increases consecutively. During the propagation of ultrasonic waves, it is necessary to overcome the heat loss caused by the internal friction of internal defects, that is, by the viscous friction effect. The propagation of ultrasonic waves in the briquette medium is a kind of energy transmission. Its propagation can also be regarded as the propagation of a stress wave. Therefore, it is accompanied with energy attenuation, which appears as a reduction in the amplitude of the received head waves. On the premise that briquette samples have the same volumetric mass, the particle size reflects the size of pores, that is, the bigger the particle size of the briquette, the larger the pores in it. This also results in larger energy consumption in propagation, leading to the above-observed results. As can be seen from Fig.14(c), as the pressure of the sample increases, the ultrasonic attenuation coefficient also decreases continuously. Under the conditions of briquettes with same mass and particle size, the ultrasonic tests under three different pressures of 6, 8 and 10 Mpa can be approximately considered as three specific states in a uniaxial compression process. With the increase of pressure, many open structural surfaces, pores and cracks, in the coal sample are compressed to close. Thus, both the number and size of these pores and cracks will be reduced, leading to the reduction of ultrasonic energy dissipation during scattering. Therefore, the scattering attenuation of the ultrasonic waves will show decreasing trend. As a result, the amplitude of the ultrasonic head waves is larger, making the calculated attenuation coefficient smaller. As can be seen from Fig.14(d), as the number of crack layers in the sample increases, the attenuation of the ultrasonic wave also increases. With the increase of the crack thickness, the reflection, refraction and diffraction of ultrasonic waves correspondingly enhance, indicating that the degree of ultrasonic scattering attenuation strengthens, resulting in great increase in the attenuation coefficient of ultrasonic waves. As can be seen from Fig.14 (e), with the increase of the crack size, the attenuation of the ultrasonic wave also increases. Larger cracks reflect more ultrasonic signals, making their diffraction more difficult and leading to an increase in attenuation. Fig.14(f) shows that with the increase of the crack dip, the ultrasonic attenuation also decreases, showing a similar changing trend to that of the ultrasonic wave velocity, indicating that ultrasonic attenuation is positively

correlated with the change in wave velocity. In addition, these two also have a common feature. When the voltage is less than 500 V, the attenuation scope of ultrasonic waves decreases sharply and when the voltage is greater than 500 V, the attenuation scope of ultrasonic waves tends to be stable. Therefore, for studies on ultrasonic attenuation, the emission voltage > 500 V is used.

3.6 Effects of different humidity on ultrasonic attenuation

Fig.15 shows the dependence of ultrasonic wave attenuation coefficient on the wetting height of, samples with different mass, particle size, crack thickness, size and dip, as well as pressures. It is clear from the figure that during the wetting process, attenuation of ultrasonic waves is different in different coal samples. In general, the ultrasonic attenuation coefficient increases with the wetting height increasing. Among them, the changes of attenuation coefficient with sample mass and particle size increasing demonstrate a similar trend, as shown in Fig.15(a) and Fig.15(b). For example, as shown in Fig.15(a), at the early stage of wetting process, the attenuation coefficient has a positive correlation with the wetting degree, reaching the peak at height of 4/5, and then beginning to fall. During the wetting process, water permeates the briquette, improving the medium for ultrasonic transmission, making ultrasonic wave more easily and quickly reach its target position, and leading to less ultrasonic wave energy lose in the propagation process, thereby reducing the attenuation of the ultrasonic energy. In addition, in the process of improving the propagation medium, water also presents some disadvantages to ultrasonic transmission. For example, when water penetrates into coal, the intermolecular distance between water extends. At this stage, the so-called water wedging effect may happen so as to increase ultrasonic attenuation. Besides, the presence of water also softens coal to promote ultrasonic attenuation. At the initial wetting stage, an increase in ultrasonic attenuation indicates that the effect of medium improvement by water is less than the sum of water wedging and softening effects. When the sample is fully wetted, the result is exactly the opposite, which explains why the curve shows a trend of increase before decrease. Moreover, the peak of attenuation coefficient increases with the increase of sample mass and lowers with the increase of the particle size. Different from Figs.15(a) and (b), the briquettes used for the experiments in Fig.15(c) are prepared under the pressure of 6, 8 and 10 MPa, much smaller than that of 20 MPa used in the first two groups of experiments. The smaller density makes water penetrate into coal more easily and quickly, facilitating the attenuation coefficient reaching the peak in advancement. Fig.15(d) clearly shows that the attenuation coefficient shows a trend of increase before decrease with the increase of the wetting degree. In addition, with the increase of crack thickness, the peak of attenuation coefficient ascends and the difference in attenuation coefficients narrows, indicating that water is able to reduce the difference in attenuation coefficient due to cracks. Fig.15(e) shows that with the increase of wetting, the attenuation coefficient shows a trend of increases first and then tends to stabilize. Fig.15(f) clearly shows that at the dry state, the dip of cracks varies from 0°–90°, and the attenuation coefficient gradually lowers. With the increase of wetting degree, all attenuation coefficients show a trend of increase before decrease, reaching its peaks at wetting height of 1/5.

To study the relationship between the ultrasonic wave velocity and its attenuation in the briquettes, the experimental data of ultrasonic attenuation and wave velocity are utilized for fitting. The fitting results shown in Figs.16 and 17 indicate that under the same conditions, the ultrasonic attenuation coefficient is negatively correlated with the mass, particle size and pressure of the specimen. Correlation between attenuation coefficient and the characters of cracks is not obvious and need to be further explored in the future. It is worthy of note that in the absence of artificial cracks in the coal sample, the ultrasonic attenuation increases with the propagation velocity increase, and their relationship is more in line with an exponential function. By contrast, in the presence of artificial cracks, the ultrasonic attenuation shows a trend of increases before decrease with the change in wave velocity and their relationship is more consistent with a power function.

4. Conclusions

The conclusions are summarized as follows:

1) Under the same conditions, a briquette sample with larger mass, smaller particle size and higher pressure is more conducive for ultrasonic signals with higher main frequency and larger amplitude to transmit in it. The ultrasonic amplitude is positively correlated with the emission voltage, and its longitudinal wave frequency is negatively correlated with the emission voltage. The wave velocity has a positive correlation with the wetting degree of the sample. Among the factors impacting wave velocity, the impact of sample mass is the greatest, followed by the particle size, and impact of the pressure is the least. At the dry stage, the wave velocity in gas coal is smaller than that in bituminous coal. At complete wetting stage, the wave velocity in gas coal is greater than that in bituminous coal.

2) At the dry stage, the effect of crack thickness on the wave velocity is small, and gradually strengthens with increase of the wetting degree, whereas the crack size behaves contrarily. The ultrasonic wave velocity in briquettes has an obvious bedding effect. At the dry stage, the ultrasonic velocity shows a gradually increasing trend with the crack dip increasing. With the increase of the wetting degree, the increment in wave velocity drops with the crack dip increasing.

3) The attenuation of ultrasonic energy during its transmission in briquettes decreases with the increase of the emission voltage. Under the same conditions, the ultrasonic attenuation decreases with particle size, crack thickness and crack size decreasing, but with the mass, the pressure and crack dip increasing, and shows a trend of increase before decrease as the wetting degree increases. In addition, the attenuation of ultrasonic wave increases with wave velocity increasing for intact samples and shows a trend of increase before decrease for cracked samples.

Declarations

Acknowledgement

The authors would like to acknowledge the support of the National Key Research and Development Program of China (No.2017YFC0805201), the National Natural Science Foundation of China(No. 51674158; 51574158; 51934004; 51974176), the Taishan Scholar Talent Advantage Unique Subject Team Support Program, the Major Program of Shandong Province Natural Science Foundation (No.ZR2018ZA0602), the Science and Technology Support Plan for Youth Innovation of Colleges and Universities in Shandong Province (No.2019KJH006), the Special fund for taishan scholars project (TS20190935).

References

Ai T, Zhang R, Liu J, et al. The space-time evolution of acoustic emission in the process of coal and rock triaxial compression fracture [J]. Journal of China Coal Society, 2011, 36 (12):2048–2057.

ALEXEEV, A., D., VASILENKO, T., A., ULYANOVA, E., V., 1999. Closed porosity in fossil coals. Fuel 78, 635–638. https://doi.org/ 10.1016/s0140-6701(99)98673-3

Birch, F., 1961. The velocity of compressional waves in rocks to 10 kilobars: 2. J. Geophys. Res. Atmos. 66. https://doi.org/10.1029/JZ066i007p02199

Cadoret, T., Marion, D., Zinszner, B., 1995. Influence of frequency and fluid distribution on elastic wave velocities in partially saturated limestones. J. Geophys. Res. Solid Earth 100, 9789. https://doi.org/10.1029/95jb00757

Cai, J.G., Zhao, J., 2000. Effects of multiple parallel fractures on apparent attenuation of stress waves in rock masses. https://doi.org/ 10.1016/s1365-1609(00)00013-7

Chen, Q., Liu, X.J., Liang, L.X., Wang, S., Yang, C., 2012. Numerical simulation of the fractured model acoustic attenuation coefficient. Chinese J. Geophys. 55, 2044–2052. https://doi.org/10.6038/j.issn.0001-5733.2012.06.026

Chen Y, Huang T, Liu E. Rock Physics [M]. Hefei: Press of University of Science and technology of China, 2009

Ciccotti, M., Almagro, R., Mulargia, F., 2004. Static and Dynamic Moduli of the Seismogenic Layer in Italy. Rock Mech. Rock Eng. 37, 229–238. https://doi.org/10.1007/s00603-003-0019-7

Fan, L.F., Ma, G.W., Li, J.C., 2012. Nonlinear viscoelastic medium equivalence for stress wave propagation in a jointed rock mass 50, 11–18. https://doi.org/ 10.1016/j.ijrmms.2011.12.008

Fan, L.F., Sun, H.Y., 2015. Seismic wave propagation through an in-situ stressed rock mass. J. Appl. Geophys. 121, 13–20. https://doi.org/ 10.1016/j.jappgeo.2015.07.002

Fan, L.F., Wang, L.J., Wu, Z.J., 2018. Wave transmission across linearly jointed complex rock masses. Int. J. Rock Mech. Min. Sci. https://doi.org/ 10.1016/j.ijrmms.2018.09.004

Fener, M., 2011. The effect of rock sample dimension on the P-wave velocity. J. Nondestruct. Eval. 30, 99–105. https://doi.org/10.1007/s10921-011-0095-7

Gaviglio, P., 1989. Longitudinal waves propagation in a limestone: The relationship between velocity and density. Rock Mech. Rock Eng. 22, 299–306. https://doi.org/10.1007/BF01262285

Gebrande H, Kern, Runnel F. Elastisity and inelasticity in landolt-bornstein numerical data and functional relationships in science and technology [C]// HELLWEGE K H. Physical Properties of Rocks. Springer-Verlag, Berlin-Heidelberg-New York, 1982.

Han, H., Wang, P., Li, Y., Liu, R., Tian, C., 2020. Effect of water supply pressure on atomization characteristics and dust-reduction efficiency of internal mixing air atomizing nozzle. Adv. Powder Technol. 31, 252–268. https://doi.org/https://doi.org/10.1016/j.apt.2019.10.017

Hudson, J.A., Pointer, T., Liu, E., 2001. Effective□edium theories for fluid□aturated materials with aligned cracks. Geophys. Prospect. 49, 509–522. https://doi.org/ 10.1046/j.1365-2478.2001.00272.x

Lebedev, M., Wilson, M.E.J., Mikhaltsevitch, V., 2015. An experimental study of solid matrix weakening in water-saturated Savonnières limestone. Geophys. Prospect. 62, 1253–1265. https://doi.org/10.1111/1365-2478.12168

Li M. Study on dynamics features of ultrasonic velocities in loading coal [D]. 2015.

Liu, J., Liu, D., Cai, Y., Gan, Q., Yao, Y., 2017. Effects of water saturation on P-wave propagation in fractured coals: An experimental perspective. J. Appl. Geophys. 144, 94–103. https://doi.org/10.1016/j.jappgeo.2017.07.001

Liu J, Sun W, Jing B A. P-wave velocity prediction in porous medium with liquid-pocket patchy saturation [J]. Applied mathematics and mechanics, 2015, 36(11):1427-1440. https://doi.org/10.1007/s10483-015-1993-7

Liu, S.Q., Sang, S.X., Liu, H.H., Zhu, Q.P., 2015. Growth characteristics and genetic types of pores and fractures in a high-rank coal reservoir of the southern Qinshui basin. Ore Geol. Rev. 64, 140–151.

Liu, Y., Lu, C.-P., Liu, B., Zhang, H., Wang, H.-Y., 2019. Experimental and field investigations on seismic response of joints and beddings in rocks. Ultrasonics 97, 46–56. https://doi.org/https://doi.org/10.1016/j.ultras.2019.05.001

Liu Z., Wang W, Yang H., et al. Experimental study on the fractal pattern of a coal body pore structure around a water injection bore [J]. Journal of Energy Resources Technology, 2020, 142(1): 012302. https://doi.org/10.1016/j.fuel.2020.117088

Liu, Z., Wang, W., Cheng, W., Yang, H., Zhao, D., 2020. Study on the seepage characteristics of coal based on the Kozeny-Carman equation and nuclear magnetic resonance experiment. Fuel 266, 117088.

https://doi.org/https://doi.org/10.1016/j.fuel.2020.117088

Ma, G.W., Fan, L.F., Li, J.C., 2013. Evaluation of equivalent medium methods for stress wave propagation in jointed rock mass. Int. J. Numer. Anal. Methods Geomech. 37, 701–715. https://doi.org/10.1002/nag.1118

Mahoney, S.A., Rufford, T.E., Johnson, D., Dmyterko, A.S.K., Rodrigues, S., Esterle, J., Rudolph, V., Steel, K.M., 2017. The effect of rank, lithotype and roughness on contact angle measurements in coal cleats. Int. J. Coal Geol. 179, 302–315. https://doi.org/10.1016/j.coal.2017.07.001

Mashinskii, E.I., 2013. Elastic-microplastic nature of wave propagation in the weakly consolidated rock. J. Appl. Geophys. 101, 11–19. https://doi.org/ 10.1016/j.jappgeo.2013.11.007

Meng Z, Liu C, He X, et al. Experimental research on acoustic wave velocity of coal measures rocks and its influencing factors [J]. Journal of Mining & Safety Engineering, 2008, 25(4):389–393.

None, n.d. Seismic visibility of fractures: Pyrak-Nolte, L J; Cook, N G W; Myer, L R Proc 28th US Symposium on Rock Mechanics, Tucson, 29 June–1 July 1987P47–56. Publ Rotterdam: A A Balkema, 1987 25, 220–224.

Pan, R.K., Cheng, Y.P., Dong, J., Chen, H.D., 2014. Research on permeability characteristics of layered natural coal under different loading and unloading. J. China Coal Soc. 39, 473-477(5). https://doi.org/10.13225/j.cnki.jccs.2013.0791

Pyrak-Nolte, L.J., Myer, L.R., Cook, N. G. W. Transmission of seismic waves across single natural fractures. J. Geophys. Res. 1990, 95:8617–8638.

https://doi.org/10.1016/0148-9062(88)90189-1

Prasad, M., Manghnani, M.H., 2002. Effects of pore and differential pressure on compressional wave velocity and quality factor in Berea and Michigan sandstones. Geophysics 62, 1163–1176. https://doi.org/10.1190/1.1444217

Shea, V.R., Hanson, D.R., 1988. Elastic wave velocity and attenuation as used to define phases of loading and failure in coal. Int. J. Rock Mech. Min. Sci. Geomech. Abstr. 25, 431–437. https://doi.org/ 10.1016/0148-9062(88)90983-7

Wang, J., Ning, J., Jiang, L., Jiang, J.-Q., Bu, T., 2018. Structural characteristics of strata overlying of a fully mechanized longwall face: A case study. J. South. African Inst. Min. Metall. 118, 1195–1204. https://doi.org/10.17159/2411-9717/2018/v118n11a10

Wang Yungang, Li Mangui, Chen Bingbing, et al. Experimental study on ultrasonic characteristics of dry and saturated watery coal samples [J]. Journal of China Coal Society, 2015, 40(10):2445–2450. https://doi.org/10.13225/j.cnki.jccs.2014.1175

Xu, X.L., Zhang, R., Dai, F., Yu, B., Zhang, Y.F., 2015. Effect of coal and rock characteristics on ultrasonic velocity. J. China Coal Soc. 40, 793–800. https://doi.org/10.13225/j.cnki.jccs.2014.3012

Zhang H. Genetic types of coal pores and their research. Journal Of China Coal Society. 2001; 26(1):40–44.https://doi.org/10.3321/j.issn:0253-9993.2001.01.009

Zhao, J., Zhao, X.B., Cai, J.G., 2006. A further study of P-wave attenuation across parallel fractures with linear deformational behaviour. Int. J. Rock Mech. Min. Sci. 43, 776–788. https://doi.org/10.1016/j.ijrmms.2005.12.007

Figures

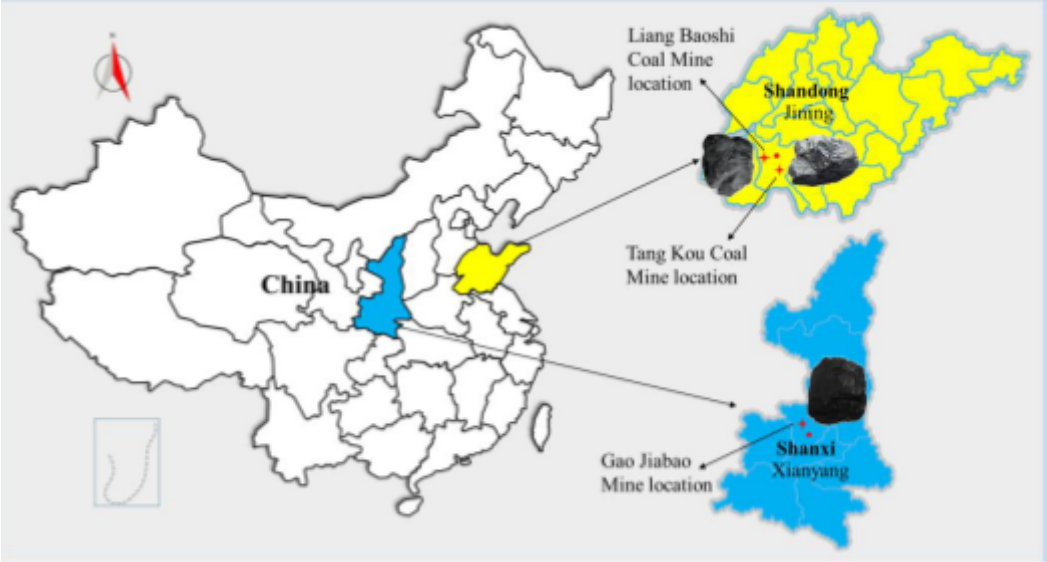

Figure 1

Map of the raw coal sampling sites Note: The designations employed and the presentation of the material on this map do not imply the expression of any opinion whatsoever on the part of Research Square concerning the legal status of any country, territory, city or area or of its authorities, or concerning the delimitation of its frontiers or boundaries. This map has been provided by the authors.

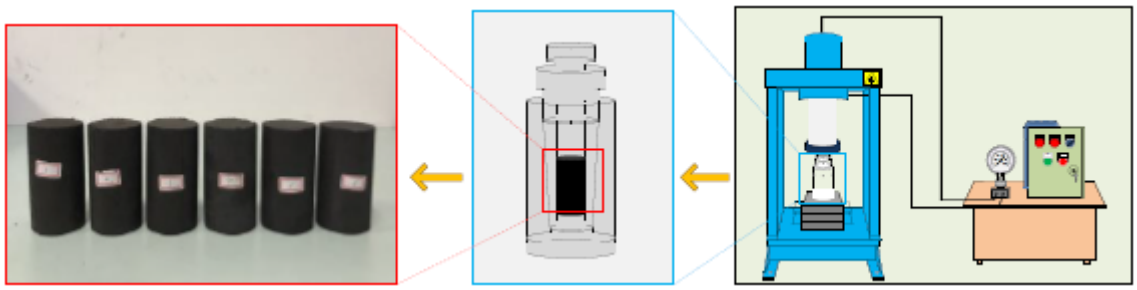

Figure 2

Procedure of briquette samples preparation

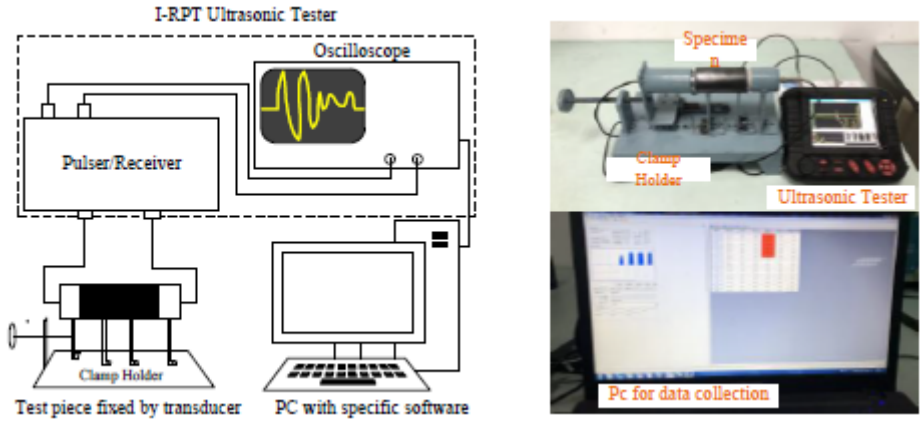

Figure 3

I-RPT ultrasonic tester for water-bearing coal samples

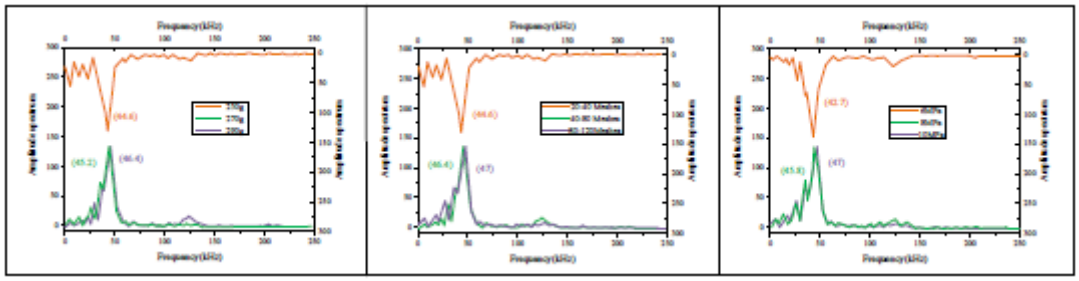

Figure 4

Effects of mass, particle size and pressure of samples on the frequency of ultrasonic waves propagating in the briquette samples

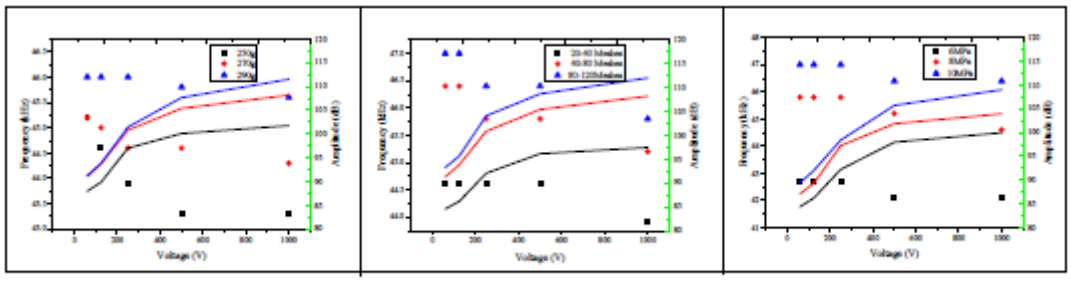

Figure 5

Dependence of different emission voltages upon acoustic amplitude and frequency

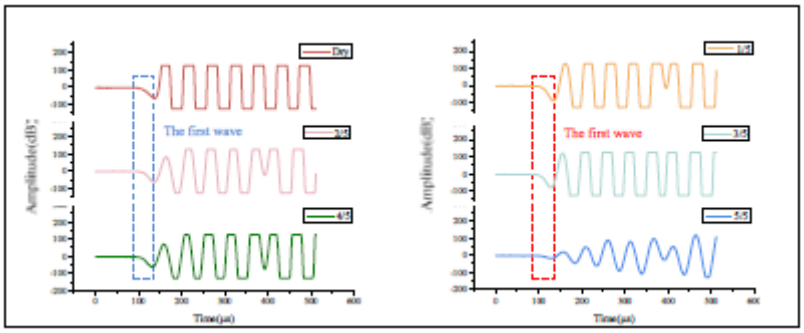

Figure 6

Oscillographs of ultrasonic waves transmitting through briquettes with different wetting height

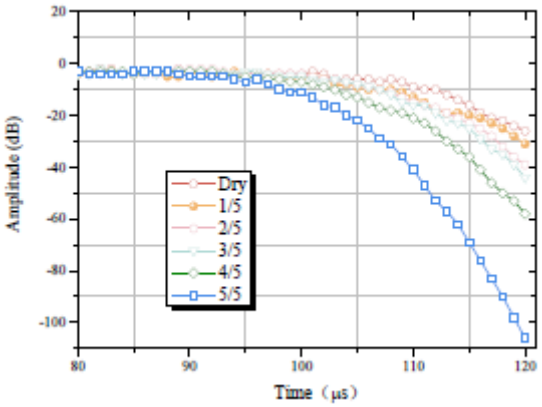

Figure 7

Oscillographs of ultrasonic head waves transmitting through briquettes with different wetting height

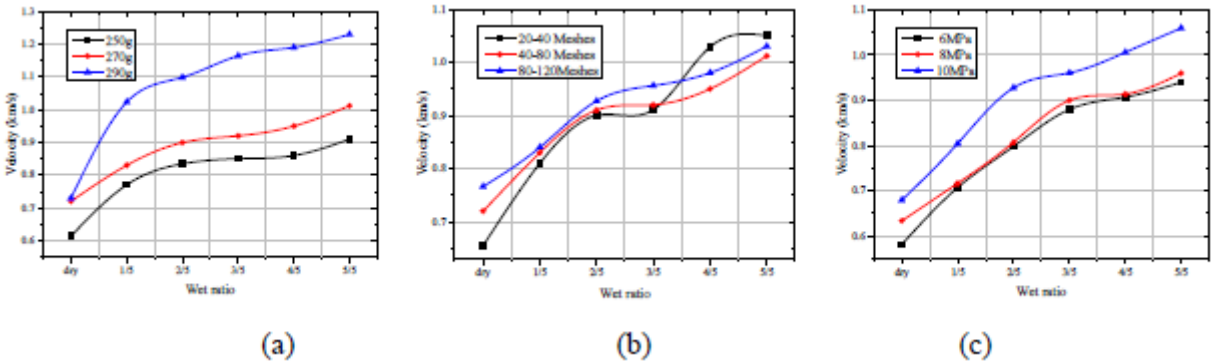

Figure 8

Dependences of acoustic velocity on different wetting heights.

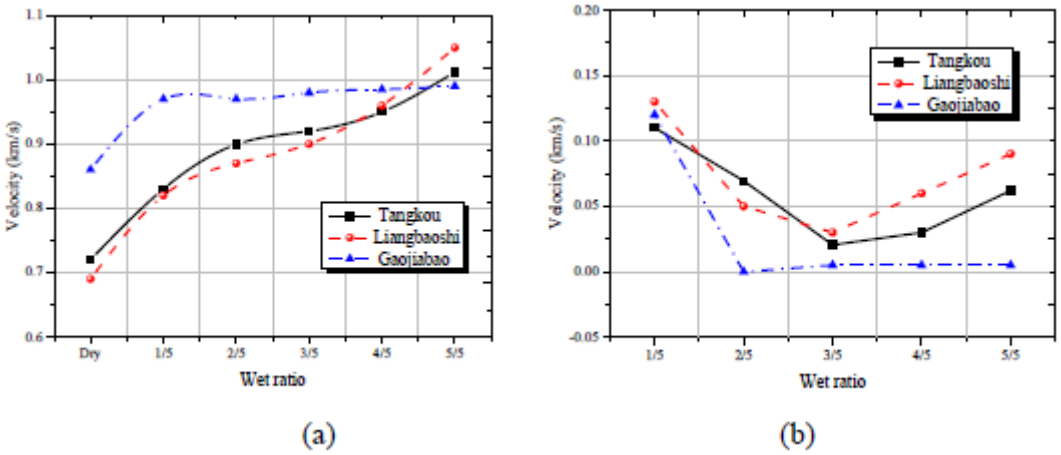

Figure 9

Relationship of ultrasonic wave velocity to wetting degree of different coal samples (a)The relationship between wetting and wave velocity of different coal samples (b)The relationship between wetting and wave velocity increment of different coal samples

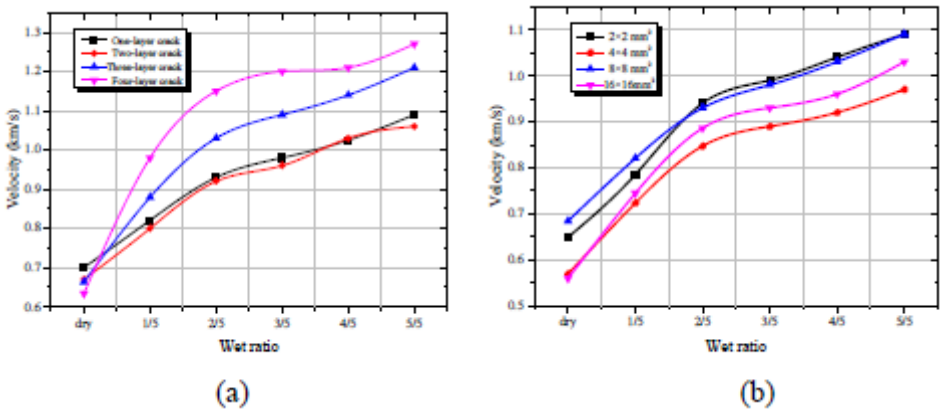

Figure 10

Effects of crack size and openness on ultrasonic velocity in briquettes at different wetting heights (a) The relationship between wetting and wave velocity under different crack thickness (b)The relationship between wetting and wave velocity under different crack sizes

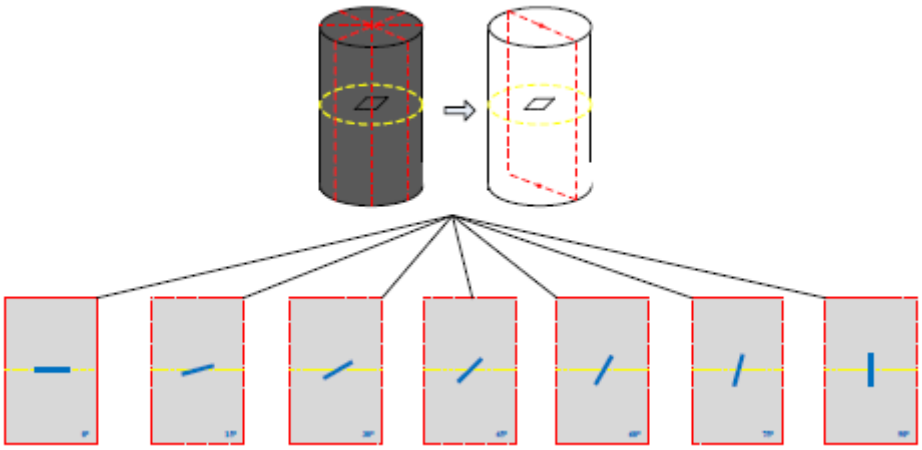

Figure 11

Schematic of artificial cracks with different dips in the coal samples

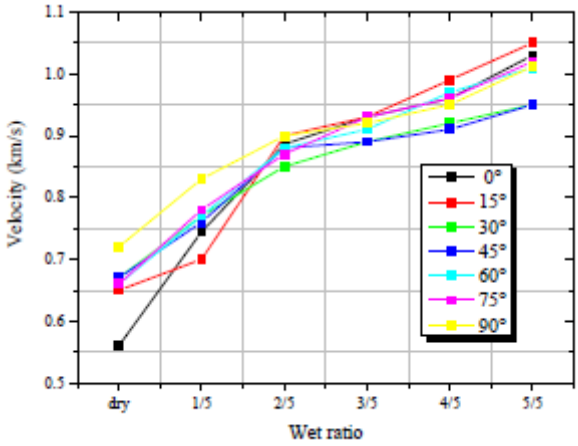

Figure 12

Effect of cracks dip on ultrasonic velocity in coal samples at wetting stage

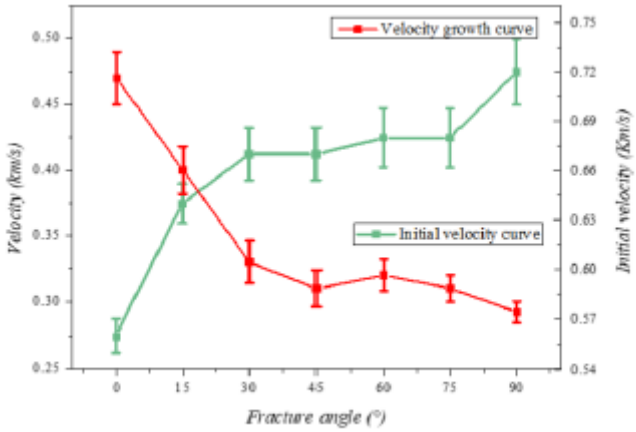

Figure 13

Velocity and velocity increment of initial ultrasonic waves in coal samples with different dips.

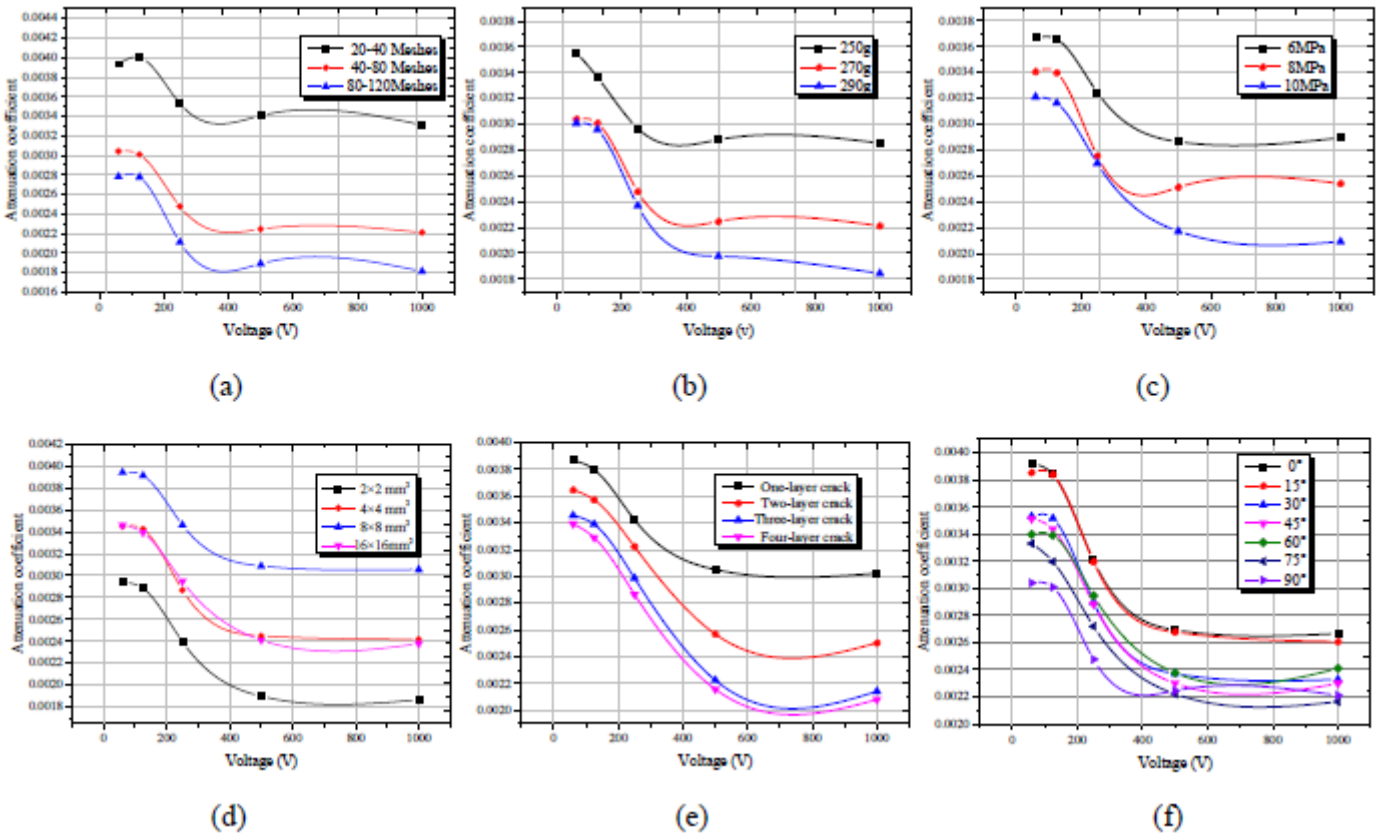

Figure 14

Dependences of ultrasonic wave attenuation upon voltage at different experimental conditions. (a) α vs. V in samples with different mass (b) α vs. V in samples with different particle sizes (c) α vs. V at in samples prepared at different pressure (d) α vs. V in samples with different crack thickness (e) α vs. V in samples with different crack size(f) α vs. V in samples with different crack dip

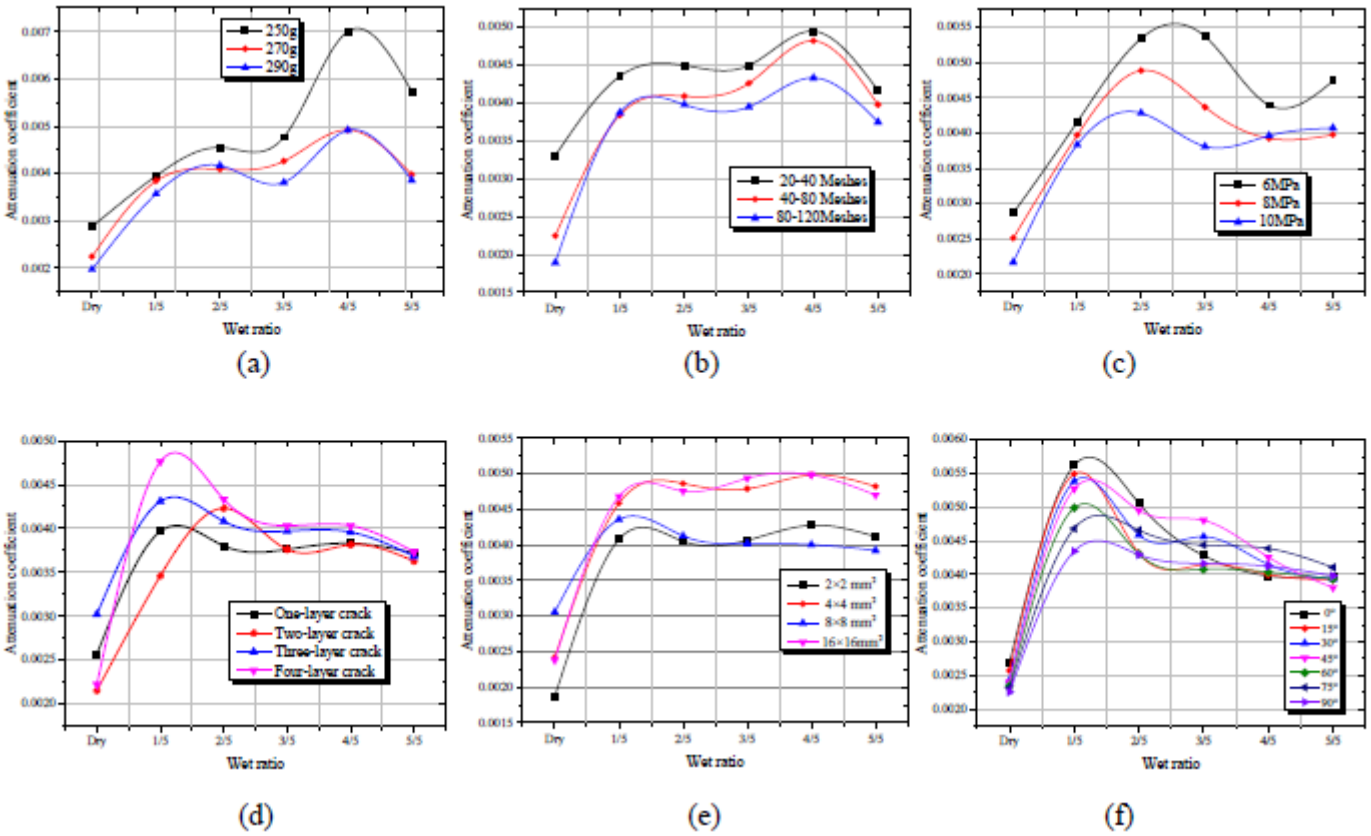

Figure 15

Effect of different wetting degrees on ultrasonic attenuation (a) α vs. V in in samples with different mass (b) α vs. V in samples with different particle size (c) α vs. V in samples prepared at different pressures (d) α vs. V in samples with different crack thickness (e) α vs. V in samples with different crack size (f) α vs. V in samples with different crack dip

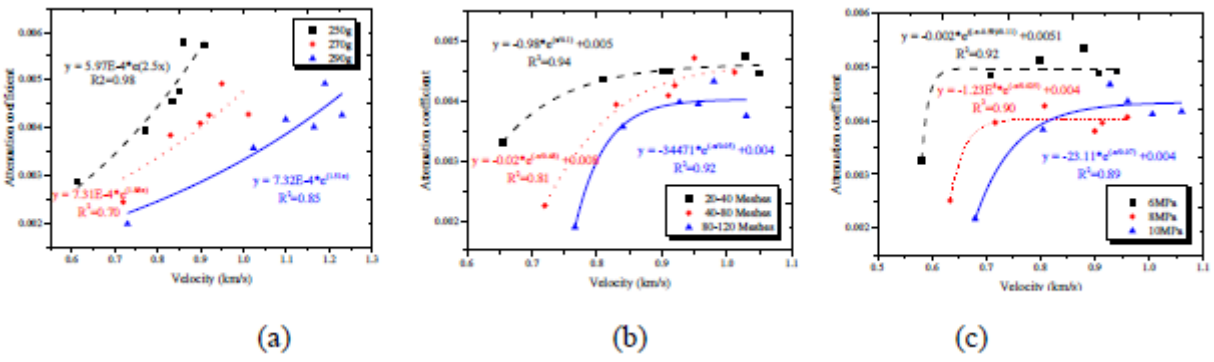

Figure 16

Relationship of ultrasonic attenuation to the wave velocity in samples without cracks (a)Relationship between velocity and attenuation of samples of different mass (b)Relationship between velocity and attenuation of samples with different particle size (c)Relationship between velocity and attenuation of samples under different pressures

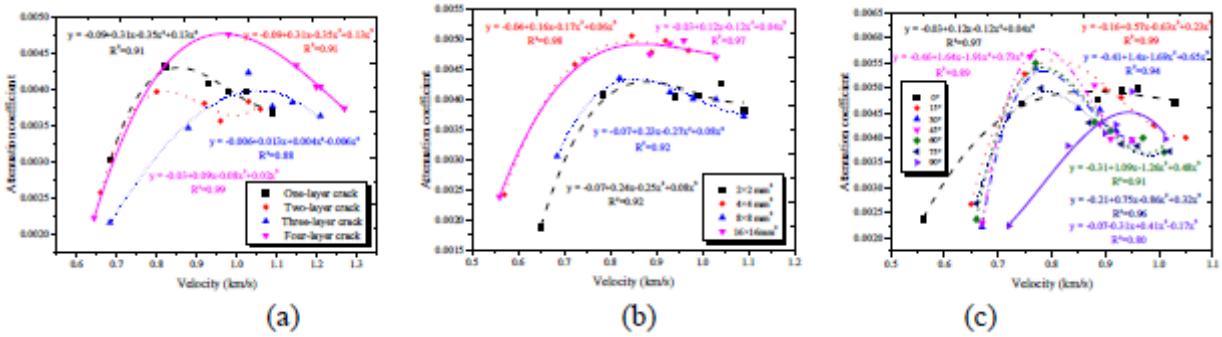

Figure 17

Relationship of ultrasonic attenuation to the wave velocity in samples with different crack thickness, particle size and dip (a)The relationship between velocity and attenuation in samples with different crack thickness (b)The relationship between velocity and attenuation of samples with different crack sizes (c)The relationship between velocity and attenuation Angle of samples with different crack inclinations